



ChemComm

Enzyme-like catalysis by single chain nanoparticles that use transition metal cofactors

Journal:	<i>ChemComm</i>
Manuscript ID	CC-COM-10-2021-005578.R1
Article Type:	Communication

SCHOLARONE™
Manuscripts

COMMUNICATION

Enzyme-like catalysis by single chain nanoparticles that use transition metal cofactors

Received 00th January 20xx,
Accepted 00th January 20xx

Thao M. Xiong,^a Edzna S. Garcia,^a Junfeng Chen,^a Lingyang Zhu,^b Ariale J. Alzona,^a Steven C. Zimmerman*^a

DOI: 10.1039/x0xx00000x

We report a modular approach in which a noncovalently cross-linked single chain nanoparticle (SCNP) selectively binds catalyst “cofactors” and substrates to increase both the catalytic activity of a Cu-catalyzed alkyne-azide cycloaddition reaction and the Ru-catalyzed cleavage of allylcarbamate groups compared to the free catalysts.

Conducting transition metal-catalyzed bioorthogonal reactions inside cells has enabled the intracellular synthesis of drugs and dyes for potential applications in therapy and imaging.^{1–3} However, most transition metal catalysts have poor water solubility and low stability in biologically relevant media. Recently reported approaches use metal nanoparticles and polymers to achieve intracellular delivery and catalysis.⁴ One solution mimics metalloenzymes by cross-linking a polymer chain around one or more metal centers to obtain single chain nanoparticles (SCNPs).^{5,6} Reported SCNP examples require covalent cross-linking or attachment of the catalyst to the polymer, which requires the synthesis of a new polymer scaffold for each reaction of interest.^{7–9} Herein we describe a simple modular approach wherein SCNPs, which are folded via hydrophobic interactions, selectively bind both the substrates and the catalyst “cofactors.” This plug-and-play cofactor strategy offers the potential for more rapidly expanding the chemist’s toolbox of transition metal-SCNPs.

Random amphiphilic copolymers have been reported by Sawamoto and coworkers¹⁰ to undergo single-chain folding in water. Knight and coworkers¹¹ recently highlighted advances in the development of protein-mimetic synthetic macromolecules, including the assembly of random amphiphilic copolymers. We synthesized random amphiphilic polymers **P1** and **P2** from precursor poly(pentafluorophenyl acrylate) (pPFPA), which was obtained from reversible addition-fragmentation chain-transfer (RAFT) polymerization (Fig. 1a).¹²

The percent conversion was monitored by ¹H NMR and the polymer was characterized by gel permeation chromatography (GPC) and ¹H NMR (SI, Fig. S1). GPC indicated a dispersity value, $\bar{D} = 1.12$ and $M_n = 27$ kDa, which corresponded to a DP of 112. The pendant activated ester groups readily undergo substitution with amines. This flexible and efficient approach to SCNPs is analogous to one developed by Palmans, Meijer, and coworkers¹³ and we have employed it for developing several artificial metalloenzymes.^{8,9} Thus, amphiphilic polyacrylamides were obtained through post-polymerization functionalization using 10-trimethyl-ammonium-1-decylamine, and either 6-(2-naphthoxy)-1-hexylamine for **P1** or hexylamine for **P2** (Fig. 1a). The hydrophilic trimethylammonium ion (NMe_3^+) groups were designed to provide water solubility whereas the decyl linker, hexyl, and naphthyl (Np) groups assist folding and provide a hydrophobic interior for substrate and cofactor binding. The target ratio of hydrophilic/hydrophobic groups was 70:30. The ratio found by ¹⁹F NMR monitoring of the reaction was 73:27 for **P1** and 77:23 for **P2**. The polymers were also characterized by ¹H NMR, which showed a hydrophilic/hydrophobic group ratio of 72:28 for **P1** and 75:25 for **P2** (SI, Fig. S2 and S3). **P1** and **P2** were purified by precipitation and dialysis and used to produce SCNPs.

Because they are not covalently cross-linked, the flexible SCNP may aggregate at higher concentrations. To test this possibility and ensure that at the working concentrations the SCNP are monomeric, we used a method typically used to measure critical micelle concentrations (CMC). The method uses Nile Red as a fluorescent probe, which does not fluoresce in polar solvents, but exhibits strong fluorescence in hydrophobic environments.¹⁴ The point at which intermolecular SCNP aggregation occurs, which we refer to as the CMC, was estimated to be 0.05 mg/mL (1.6 μM) for **P1**. This concentration was determined from the point at which fluorescence intensity increases exponentially, indicating the assembly of multi-chain aggregates. Although we use the term CMC, the structure of the aggregates is not known. Nonetheless, we expect SCNPs to form and be monomeric at polymer concentrations below the CMC.

A 1 μM solution of **P1** was characterized by dynamic light scattering (DLS) (SI, Fig. S4). A major peak at 6.4 ± 1.1 nm was observed (size distribution by volume), indicating the main

^aDepartment of Chemistry, University of Illinois at Urbana-Champaign, Urbana, Illinois 61801, United States.

^bNMR Laboratory, School of Chemical Sciences, University of Illinois at Urbana-Champaign, Urbana 61801, United States.

*E-mail: sczimmer@illinois.edu

Electronic Supplementary Information (ESI) available. See

DOI: 10.1039/x0xx00000x

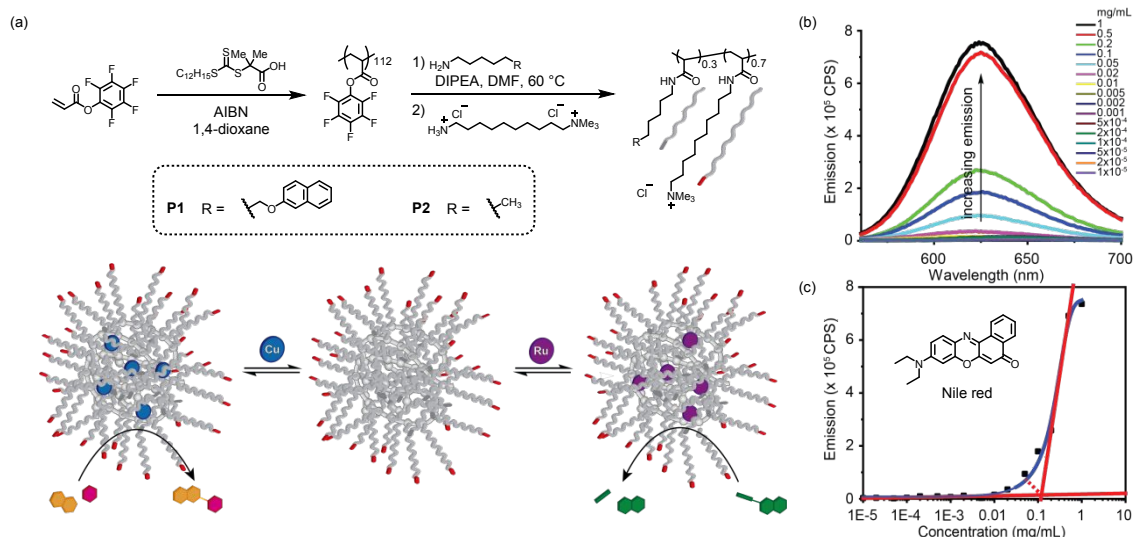


Fig. 1 (a) Synthetic scheme for **P1** and **P2** using radical polymerization and post-polymerization functionalization of pPFPA. (b) Plot of fluorescence emission vs wavelength for Nile red with 1 mg/mL (33 μM) to 10 ng/mL (330 pM) **P1** in water. (c) Plot of Nile red fluorescence emission (λ_{em} = 619 nm) vs polymer concentration. [Nile red] = 1 μM.

species present are SCNPs with a relatively small average hydrodynamic diameter consistent with previously reported SCNPs of comparable M_n .¹⁵ Characterization by diffusion ordered spectroscopy (DOSY) gave a hydrodynamic diameter of 5.7 nm, which is within error of the DLS value (SI, Fig. S5). Performing the same studies for **P2** we obtained a CMC of 0.13 mg/mL (4.3 μM) (SI, Fig. S6 and S7) and a hydrodynamic diameter of 6.2 ± 1.0 nm by DLS (SI, Fig. S8) and 6.4 nm by DOSY (SI, Fig. S9). The catalytic studies described below used a 1 μM solution of the amphiphilic polymer.

To explore the potential of **P1** and **P2** to increase the activity of transition metal catalyst cofactors, we focused first on the CuAAC, a robust reaction that proceeds under mild conditions. Wu reported biocompatible tris(triazolylmethyl)amine ligands with a bulky *tert*-butyl (tBu) substituent on two of the triazole rings to give very fast rates and minimize byproducts.^{16,17} Based

The catalytic activity of Cu-L1 and Cu-L2 with **P1** and **P2** was studied using the cycloaddition of azidocoumarin **1** and ethynylbenzene **2** (Fig. 2a). Compound **1** is non-fluorescent but formation of the triazole ring activates the fluorescence of coumarin.^{18,19} By using fluorescence as a “turn on” property, the progress of the cycloaddition reaction with Cu-L1 and Cu-L2 was readily monitored by fluorescence spectroscopy (Fig. 2b,c).

Polymer **P1** or **P2**, Cu catalyst, sodium ascorbate (NaAsc), **1**, and **2** were added to PBS buffer, and fluorescence emission curves of the cycloaddition reaction collected over 30 min (Fig. 2c). In the presence of **P1** and Cu-L1, 86% conversion was observed after 15 min compared to **P2** and Cu-L1 with 66% conversion. Free Cu-L1 achieved 13% conversion. Lower activity was observed with Cu-L2 in the presence of **P1** (26% conversion) and **P2** (12% conversion). Control reactions with **P1** or **P2** without catalyst did not generate an increase in fluorescence, indicating that the polymers alone are not active (SI, Fig. S10). The faster initial rate of reaction and higher percent conversion the catalyst-SCNP combination can be rationalized by the binding of both substrates and catalyst within the SCNP, achieving high local concentrations of each. Previous work in our group, in which a Cu-SCNP catalyzes the CuAAC reaction between **1** and different alkynes, has demonstrated that substrates with increasing aliphatic chain length and negatively charged substrates resulted in faster initial rates of reaction.⁸ The SCNP may also help protect the catalyst from side reactions that occur in the bulk environment.^{20,21} Because higher catalytic activity was observed with **P1**, subsequent studies used **P1**.

To obtain evidence for catalyst binding to the amphiphilic polymer, Nuclear Overhauser Effect Spectroscopy (NOESY) was performed.²² We first identified proton peaks with unique chemical shifts in the ¹H NMR spectra of **P1** and **L1**. The experiment was conducted without Cu because the addition of paramagnetic Cu(II) led to broadened signals such that the ligand was not observed. The ¹H NMR spectrum of **P1** has distinct and well-resolved peaks at δ 0.9–1.8 ppm (polymer

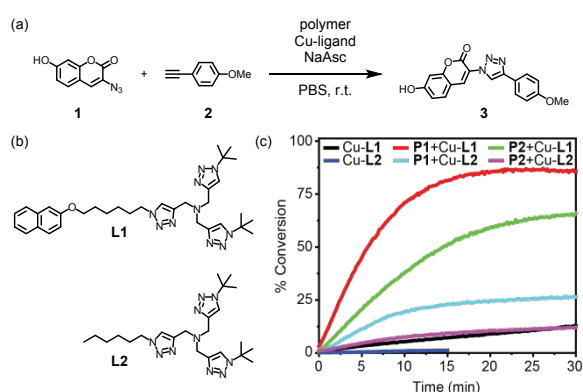


Fig. 2 (a) CuAAC activity was measured by reaction between **1** (20 μM) and **2** (40 μM) with **P1** or **P2** (1 μM), Cu catalyst (5 μM), and NaAsc (2 mM). (b) Structures of bis(*tert*-butyltriazolyl) ligands **L1** and **L2**. (c) Increase in fluorescence emission intensity at λ_{em} = 480 nm of CuAAC in PBS buffer vs. time.

on this work, we prepared ligand **L1** with a naphthyloxyhexyl side chain and ligand **L2** with a simple hexyl side chain (Fig. 2b).

backbone and alkyl side chains) and at δ 3.1 ppm ($^1\text{NMe}_3$ groups). The ^1H NMR spectrum of **L1** has distinct peaks at δ 1.6 ppm (tBu groups) and at δ 7.9 ppm (triazole rings) (SI, Fig. S11). NOESY of **P1** was conducted and cross-peaks were observed from the $^1\text{NMe}_3$ and Np groups to the polymer backbone and alkyl side chains (SI, Fig. S12). These cross-peaks are consistent with through-space interactions between protons on the amphiphilic polymer that may arise from intramolecular folding and aggregation. No cross-peaks were observed for **L1** alone (SI, Fig. S13). When **L1** was added to **P1**, new cross-peaks were observed between the ligand triazole rings and both the polymer backbone and alkyl side chains (SI, Fig. S14). Unfortunately, the signal-to-noise required the concentration of **P1** in each of the NOESY experiments to be above the CMC, but the data does indicate the potential both for intramolecular folding of **P1** and its interaction with **L1**. NOESY was also conducted for **P1** and **L2** (SI, Fig. S15), however, no new distinguishable cross-peaks were observed.

Another technique to observe and quantify binding is saturation-transfer difference (STD) NMR.²³ STD NMR has been used for ligand screening and characterization of protein binding. A practical advantage of this technique in the present case was the ability to work below the CMC. In the *off-resonance* spectrum with 1 μM **P1** and 250 μM **L1**, the ligand proton peaks undergo a slight chemical shift. DOSY was conducted to determine whether the ligand proton peaks correspond to free ligand or bound ligand (SI, Fig. S16). We observe a 100% difference between the polymer and ligand diffusion coefficients, but the smaller than expected diffusion coefficient of the ligand suggests that this value reflects an average of bound ligand and free ligand.

STD NMR was conducted with peak irradiation at δ 0.4 ppm

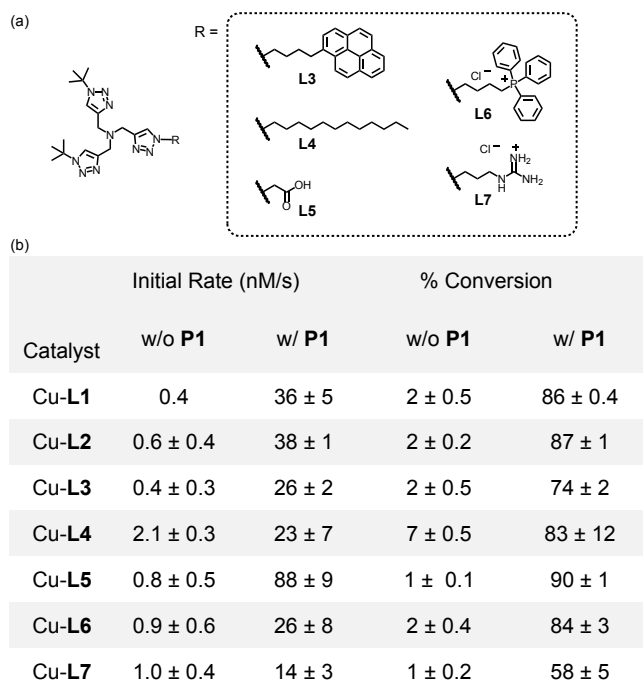


Fig. 3 (a) Library of bis(*tert*-butyltriazolyl) ligands. (b) Observed percent conversions and initial rates obtained from fluorescence emission curves of **L1** to **L7** in water. Std dev. calculated from $n = 3$.

with 1, 2, 3, 4, and 5 s saturation time (SI, Fig. S17). The STD amplification factor (A_{STD}), which can be depicted as the average number of ligands saturated per polymer, was calculated for triazole and tBu proton peaks at δ 7.7 and δ 1.4 ppm, respectively (SI, Fig. 18). The triazole proton peak has a low signal-to-noise ratio and as a result integration of this peak may have produced inflated values. In general, we obtained A_{STD} equal to the molar ratio of ligand in excess relative to the polymer with saturation times greater than or equal to 2 s. We attempted to map the ligand moieties important for interaction, which is calculated by setting the largest A_{STD} to 100% and calculating other A_{STD} with the same saturation time accordingly (SI, Fig. S19). Taking into consideration possible error with the triazole proton, the triazole and tBu protons are in similar proximity to the polymer. However, we were unable to map the ligand Np protons because of chemical shift overlap with the polymer Np protons.

We observed by NOESY and STD NMR that **L1** binds to the polymer via the tBu substituted triazole rings. To study how the structure of the third side chain affects interactions with the SCNP and CuAAC catalysis, we synthesized additional ligands **L3** to **L7** (Fig. 3a). The library included neutral ligands **L1** to **L4**, anionic ligand **L5**, and cationic ligands **L6** to **L7**, and their catalytic activity was again analyzed using the fluorogenic click reaction in Fig. 2a. Polymer **P1**, Cu catalyst, NaAsc, **1**, and **2** were added to water, and fluorescence emission curves of the cycloaddition reaction were obtained over 15 min (Fig. 3b). The largest enhancement in initial rate and percent conversion was observed for **L5** (BTAA), which is anionic under the working conditions. We rationalize that it may bind tighter to the positively-charged SCNP through favorable electrostatic interactions.²⁴ The cationic ligands performed the worst in the presence of **P1** but still demonstrated higher activity than the free catalysts. In comparison, a moderate improvement in initial rate and percent conversion was observed for the more hydrophobic ligands, consistent with their tighter binding to the hydrophobic pockets of the SCNP and a resultant higher local concentration seen by the alkyne and azide substrates.

We demonstrated the plug-and-play cofactor approach of our system by conveniently generating a structure-activity relationship using different Cu catalysts. To extend this approach, we sought to use a second transition metal catalyst as a cofactor for **P1**. We were attracted to the Ru-catalyzed cleavage of allylcarbamate groups as a widely used bioorthogonal reaction that can be utilized to generate fluorophores from non-fluorescent precursors and active drugs from pro-drugs. Tanaka and coworkers reported the first example of a Ru catalyst for the cleavage of *N*-allyloxycarbonyl groups.²⁵ In 2017, the Meggers group optimized the Ru catalyst and demonstrated its catalytic activity under biologically relevant conditions.²⁶

Ru-**L8** was prepared as reported²⁶ and Ru-**L9** was prepared from 6-(naphthalen-2-yloxy)hexan-1-amine (Fig. 4b and SI). Evaluation of their catalytic activity used *N*-allyloxycarbonyl-caged coumarin **4** as a fluorogenic reporter (Figure 4a).²⁷ The caged substrate is non-fluorescent but cleavage of the allylcarbamate group results in fluorescence. Polymer **P1**, Ru

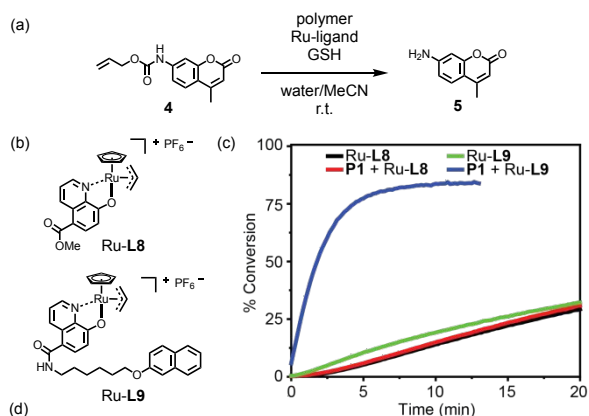


Fig. 4 (a) Ru-catalyzed cleavage of allylcarbamate groups was measured by the deprotection of **4** (20 μ M) with **P1** (1 μ M), Ru catalyst (5 μ M), and GSH (300 μ M). (b) Structures of catalysts Ru-L8 and Ru-L9. (c) Increase in fluorescence emission intensity at $\lambda_{em} = 440$ nm in water vs. time. (d) Observed percent conversions and initial rates obtained from kinetic study. Std dev. calculated from $n = 3$.

catalyst, glutathione (GSH), and **4** were added to water and fluorescence emission curves collected over 20 min (Fig. 4c). GSH was chosen as the reducing agent because of its biocompatibility and bioavailability. The catalytic activity of Ru-L8 did not change significantly with and without **P1** (Fig. 4d). In contrast, the catalytic activity of Ru-L9 significantly increased in the presence of **P1** with observed percent conversion increasing from 30% to 84% conversion and initial rate increasing more than 16-fold. These results are consistent with the trends we observed with the Cu catalysts where catalysts modified with hydrophobic side chains increased both the percent conversion and the initial rate with **P1** in comparison to free catalysts.

In summary we have developed a modular approach to transition metal-SCNPs that features a folded amphiphilic polymer that binds transition metal catalyst cofactors in a plug-and-play approach. This simple and versatile system was utilized to generate different Cu-SCNPs for the CuAAC reaction and Ru-SCNPs for the cleavage of allylcarbamate groups. Faster initial rates of reaction and higher percent conversions were observed for catalysts with hydrophobic or anionic ligands in the presence of the SCNPs compared to free catalysts. In addition, important ligand moieties for binding to the polymer were identified by NOESY and STD NMR. The structure of the catalyst can be optimized to increase binding to the polymer and increase initial rates of reaction in the presence of the SCNPs. The transition metal-SCNP functions under mild conditions and has potential to be used for biological applications such as therapy or diagnostics.

There are no conflicts to declare.

Acknowledgements

We thank the National Science Foundation (NSF CHE-1709718) for funding. We also thank D. Olson and N. Duay for assistance with the NMR studies.

Notes and references

- 1 K. Lang and J. W. Chin, *ACS Chem. Biol.*, 2014, **9**, 16-20.
- 2 D. M. Patterson, L. A. Nazarova and J. A. Prescher, *ACS Chem. Biol.*, 2014, **9**, 592-605.
- 3 J. Li and P. R. Chen, *Nat. Chem. Biol.*, 2016, **12**, 129-137.
- 4 Y. Bai, J. Chen and S. C. Zimmerman, *Chem. Soc. Rev.*, 2018, **47**, 1811-1821.
- 5 H. Rothfuss, N. D. Knofel, P. W. Roesky and C. Barner-Kowollik, *J. Am. Chem. Soc.*, 2018, **140**, 5875-5881.
- 6 J. P. Cole, C. K. Lyon and E. B. Berda, in *Bio-inspired Polymers*, ed. N. Bruns and A. F. M. Kilbinger, Royal Society of Chemistry, Cambridge, 2017, 4, 107-140.
- 7 Y. Bai, X. Feng, H. Xing, Y. Xu, B. K. Kim, N. Baig, T. Zhou, A. A. Gewirth, Y. Lu, E. Oldfield and S. C. Zimmerman, *J. Am. Chem. Soc.*, 2016, **138**, 11077-11080.
- 8 J. Chen, J. Wang, Y. Bai, K. Li, E. S. Garcia, A. L. Ferguson and S. C. Zimmerman, *J. Am. Chem. Soc.*, 2018, **140**, 13695-13702.
- 9 E. S. Garcia, T. M. Xiong, A. Lifschitz and S. C. Zimmerman, *Polym. Chem.*, 2021, DOI: 10.1039/D1PY01255J.
- 10 T. Terashima, T. Sugita, K. Fukae and M. Sawamoto, *Macromolecules*, 2014, **47**, 589-600.
- 11 M. H. Barbee, Z. M. Wright, B. P. Allen, H. F. Taylor, E. F. Pattenon and A. S. Knight, *Macromolecules*, 2021, **54**, 3585-3612.
- 12 A. Das and P. Theato, *Macromolecules*, 2015, **48**, 8695-8707.
- 13 Y. Liu, T. Pauloehr, S. I. Presolski, L. Albertazzi, A. R. A. Palmans and E. W. Meijer, *J. Am. Chem. Soc.*, 2015, **137**, 13096-13105.
- 14 J.-R. Daban, M. Samsó and S. Bartolomé, *Anal. Biochem.*, 1991, **199**, 162-168.
- 15 J. A. Pomposo, J. Rubio-Cervilla, A. J. Moreno, F. Lo Verso, P. Bacova, A. Arbe and J. Colmenero, *Macromolecules*, 2017, **50**, 1732-1739.
- 16 D. Soriano del Amo, W. Wang, H. Jiang, C. Besanceney, A. C. Yan, M. Levy, Y. Liu, F. L. Marlow and P. Wu, *J. Am. Chem. Soc.*, 2010, **132**, 16893-16899.
- 17 C. Besanceney-Webler, H. Jiang, T. Zheng, L. Feng, D. Soriano del Amo, W. Wang, L. M. Klivansky, F. L. Marlow, Y. Liu and P. Wu, *Angew. Chem. Int. Ed. Engl.*, 2011, **50**, 8051-8056.
- 18 K. Sivakumar, F. Xie, B. M. Cash, S. Long, H. N. Barnhill and Q. Wang, *Org. Lett.*, 2004, **6**, 4603-4606.
- 19 Z. Zhou and C. J. Fahrni, *J. Am. Chem. Soc.*, 2004, **126**, 8862-8863.
- 20 M. Artar, E. R. J. Souren, T. Terashima, E. W. Meijer and A. R. A. Palmans, *ACS Macro Lett.*, 2015, **4**, 1099-1103.
- 21 Y. Liu, P. Turunen, B. F. M. De Waal, K. G. Blank, A. E. Rowan, A. R. A. Palmans and E. W. Meijer, *Mol. Syst. Des. Eng.*, 2018, **3**, 609-618.
- 22 D. Neuhaus and M. P. Williamson, *The Nuclear Overhauser Effect in Structural and Conformational Analysis*, Wiley-VCH, New York, 2000.
- 23 A. Viegas, J. Manso, F. L. Nobrega and E. J. Cabrita, *J. Chem. Educ.*, 2011, **88**, 990-994.
- 24 J. Chen, J. Wang, K. Li, Y. Wang, M. Gruebele, A. L. Ferguson and S. C. Zimmerman, *J. Am. Chem. Soc.*, 2019, **141**, 9693-9700.
- 25 S. Tanaka, H. Saburi, T. Murase, M. Yoshimura and M. Kitamura, *J. Org. Chem.*, 2006, **71**, 4682-4684.
- 26 T. Völker and E. Meggers, *ChemBioChem*, 2017, **18**, 1083-1086.
- 27 T. Volker, F. Dempwolff, P. L. Graumann and E. Meggers, *Angew. Chem. Int. Ed. Engl.*, 2014, **53**, 10536-10540.